Prediction of solution structures of the Ca2+-bound γ- carboxyglutamic acid domains of protein S and homolog growth arrest specific protein 6: Use of the particle mesh Ewald method

5 AUTHORS, INCLUDING:

Prediction of Solution Structures of the Ca^{2+}-Bound γ-Carboxyglutamic Acid Domains of Protein S and Homolog Growth Arrest Specific Protein 6: Use of the Particle Mesh Ewald Method

Lalith Perera,* Leping Li,# Tom Darden,# D. M. Monroe,§ and Lee G. Pedersen*#

*Department of Chemistry, University of North Carolina, Chapel Hill, North Carolina 27599-3290; #National Institute of Environment Health Science, Research Triangle Park, North Carolina 27709; and §Department of Medicine, University of North Carolina, Chapel Hill, North Carolina 27599-7295 USA

ABSTRACT   The solution structures of the N-terminal domains of protein S, a plasma vitamin K-dependent glycoprotein, and its homolog growth arrest specific protein 6 (Gas6) were predicted by molecular dynamics computer simulations. The initial structures were based on the x-ray crystallographic structure of the corresponding region of bovine prothrombin fragment 1. The subsequent molecular dynamics trajectories were calculated using the second-generation AMBER force field. The long-range electrostatic forces were evaluated by the particle mesh Ewald method. The structures that stabilized over a 400-ps time interval were compared with the corresponding region of the simulated solution structure of bovine prothrombin fragment 1. Structural properties of the γ-carboxyglutamic acid (Gla) domains obtained from simulations and calcium binding were found to be conserved for all three proteins. Analysis of the predicted solution structure of the Gla domain of Gas6 suggests that this domain should bind with negatively charged phospholipid surfaces analogous to bovine prothrombin fragment 1 and protein S.

INTRODUCTION

Protein S, a plasma vitamin K-dependent glycoprotein, is a cofactor of the anticoagulant protease, activated protein C (APC) (Walker, 1981, 1984; Lundwall et al., 1986; Sugo et al., 1986). Coagulation factors Va and VIIIa, which are essential for the catalytic activity of the prothrombinase and tenase complexes, respectively, are effectively inactivated by APC in the presence of protein S. Protein S is considered to function as a receptor of APC on the phospholipid surface in the anticoagulation process. It has been reported that protein S inhibits factor Xa directly (Heeb et al., 1994) and competes with prothrombin for direct binding to factor Va (Heeb et al., 1993), thereby indirectly inhibiting prothrombin's binding to factor Va. This inhibitory activity is independent of APC. In plasma, half of the protein S complexes with the C4b-binding protein (C4bBP) in a noncovalent complex that results in the loss of the APC cofactor function of protein S (Dahlback, 1986; Greengard et al., 1995). Even though the exact function of this complex is unknown, it is believed that protein S provides a membrane-binding site for the accumulation of C4bBP near the cell surface, thereby preventing complement-mediated cellular damage (Esmon and Fukudome, 1995). In addition to its functionality in the process of coagulation, protein S may also play a role in regulating cell proliferation (Esmon, 1995).

Protein S has also been identified as a mitogen for smooth muscle cells. In recent experiments, Stitt et al. (1995) identified bovine and human protein S as ligands for murine tyrosine kinase receptors (e.g., Rse and Axl) whose extracellular domain resembles neutral cell adhesion molecules. These findings were based on the protein's apparent ability to activate the kinase. However, later experiments showed that human protein S fails to activate human Rse (Varnum et al., 1995; Godowsky et al., 1995; Mark et al., 1996). Instead, another protein, growth arrest specific protein 6 (Gas6), which was initially identified as a product of a gene whose expression is increased in fibroblasts upon growth arrest, acts as a ligand for human Rse and stimulates receptor tyrosine kinase (Godowsky et al., 1995; Mark et al., 1996; Ohashi et al., 1995). Gas6 was also reported to function as a potentiating factor for thrombin-induced proliferation of vascular smooth muscle cells (Nakano et al., 1995), a critical event in the thickening of the vascular walls accompanying artherosclerosis or restenosis.

Surprisingly, Gas6 has a high homology (43% overall identity) to protein S and consists of the same domains identified in protein S (a γ-carboxyglutamic acid (Gla) domain, followed by four epidermal growth factor-like domains, followed by a sex hormone binding globulin-like domain; Lundwall et al., 1986; Dahlback et al., 1986, 1990; Manfioletti et al., 1993). The Gla domain, present in the family of vitamin K-dependent proteins, is required for the calcium-dependent phospholipid binding that mediates the interaction of these proteins with cellular membranes (Hayashi et al., 1995). In a study to elucidate the growth-potentiating activity of Gas6, Nakano et al. (1995) detected 11.7 Gla residues/mol after alkaline hydrolysis, thus indicating that Gas6 is also a vitamin K-dependent protein. These Gla residues were thought to be involved in the Ca^{2+} binding found to be essential for the conformation and functionality of Gas6 in its binding to Axl (Ohashi et al., 1995; Nakano et al., 1997). The mitogenic activity of Gas6,

found in an experiment involving growth arrest by serum starvation, was ascribed to the interaction of Gas6 with Axl tyrosine kinase (Goruppi et al., 1996). However, in a study with deleted variants of Gas6, Mark et al. (1996) concluded that the Gla domain and the epidermal growth factor-like domains of this protein are not involved in the receptor binding. Interestingly, to date there has been no established link between Gas6 and the blood coagulation process.

In the present study, the molecular dynamics simulation technique has been used as a tool to estimate atomic-level structural information on the solvated Gla domains of protein S and its homolog Gas6. The predicted structures are first compared with the simulated solution structure of bovine prothrombin fragment 1 (BF1), the crystal structure of which was recently established (Soriano-Garcia et al., 1992). Because the Gla domain of protein S binds to negatively charged phospholipids (Schwalbe et al., 1989, 1990), direct comparison of the results from our molecular dynamics simulations can reasonably be used to assess the phospholipid binding affinity of Gas6. We have included a stretch of amino acids beyond the Gla domain for both Gas6 and protein S in the present work; however, our focus is on the properties associated with the Gla domains.

The amino acid sequences of the selected portions of the proteins used in the present simulations are shown in Fig. 1. The necessity for the reevaluation of the BF1 system arose because the previous trajectory calculations of this protein (Hamaguchi et al., 1992) were carried out with the first generation of the AMBER force field (Weiner et al., 1984, 1986), in conjunction with a twin-range cutoff method to incorporate long-range forces. We now employ the most recent AMBER force field (Cornell et al., 1995) and the accurate particle mesh Ewald (PME) method (Essmann et al., 1995) for evaluating electrostatics. In the present trajectory calculations of BF1, we have limited the number of amino acid residues to 145, which includes the kringle domain, to facilitate a direct comparison of BF1 with the previous calculations.

MATERIALS AND METHODS

Model construction

The initial structures of the model proteins were derived from the crystallographic coordinates of BF1/Ca fragment 1 (Soriano-Garcia et al., 1992) by using SYBYL6.0 (Tripose Associates, St. Louis, MO). Necessary side chains and hydrogen atoms were added to the x-ray crystallographic structure, followed by energy minimization using a distance-dependent dielectric function. To obtain the correct amino acid sequence, the residues

of BF1 that were different from protein S and Gas6 were mutated by changing only the side-chain atoms; i.e., the coordinates of homologous residue atoms and backbone atoms were retained. The side-chain replacement procedure implemented in SYBYL uses only information on most commonly occurring (in the data base of crystallized proteins) side-chain rotamers. Unacceptable van der Waals contacts were avoided by performing side-chain conformational searches, and where possible, the original BF1 crystallographic water molecules were preserved. The original positions of the calcium ions were unchanged when the protein S and Gas6 were created from the crystal structure of BF1. This was certainly feasible, because all of the positions of Gla residues present in BF1 were found to be conserved in the other two proteins used in this study. In the case of Gas6, to achieve neutrality in the segment of interest (residues 1–73), two additional Ca^{2+} ions (nine total) were placed near Gla^{32} and Gla^{36} as malonate-chelation complexes. The loop regions following the Gla domain were constructed by implementing an arbitrary but well-defined procedure. In the first step of this procedure, the two cystines (Cys^{48} and Cys^{61}) that bracket the "thumb loop" in BF1 were used as anchors for loop residues, while all residues between them were deleted. Three new amino acid residues were introduced between the anchor residues by the loop search method in the SYBYL6.0 biopolymer package (Tripos Associates). The region between these two cystine residues was then subjected to energy minimization while the other residues were held fixed. The third added residue was deleted and the two neighboring residues of the deleted residue were then selected to be the new anchors. Three new residues were added by the loop search method, followed by the energy minimization of the newly created "thumb loop" (a closed loop at each step). This procedure was continued until the complete "thumb loop" was constructed. In the minimization steps, all residues added between the two anchor cystine residues were allowed to move in the force field provided by the first 46 stationary residues.

Simulation procedure

In the previous molecular dynamics simulations of BF1 (Hamaguchi et al., 1992), the first generation of the AMBER force field was used. Long-range interactions were computed by a twin-range cutoff method. The second generation of the AMBER force field, in conjunction with the PME method to accommodate long-range interactions, was used in the present study to recalculate the trajectories for BF1. For completeness, we have chosen to use the same number of residues (1–145) for BF1 as was used in the work of Hamaguchi et al. (1992). The system contained ~8000 water molecules. After 50 ps of initial constant volume dynamics, the trajectories were extended to another 262 ps at constant pressure.

The structures of protein S and Gas6 were reminimized in vacuum (crystallographic water molecules present) by using the second generation of AMBER force field (Cornell et al., 1995) with a distance-dependent dielectric function. In this energy minimization step, the amino acid residues 1–47 were initially held fixed while the loop region was minimized. This minimization step consisted of 100 steepest descent steps followed by 10,000 steps of conjugate gradient minimization. The whole system was then subjected to energy minimization (100 steps of steepest descent minimization followed by 15,000 steps of conjugate gradient minimization). After the energy minimization in vacuum, the proteins with the crystallographic water molecules were placed in a box of TIP3P water molecules. The box dimensions were selected so that each side of the box

	1	10	20	30	40					
BF1	ANKGF	LXXVR	KGNLX	RXCLX	XPCSR	XXAFX	ALXSL	SATDA	FWAKY	TA CESARNPREKLNE	CLEGN
Protein S	AN.TL	LXXTK	KGNLX	RXCIX	XLCNK	XXARX	IFXNN	PXTEY	FYPKY	LG CLGSFRAGLFTAARLSTNAYPDLRS	CVNAIS
Gas6	AF.QV	FXXAK	QGHLX	RXCVX	XLCSR	XXARX	VFXND	PXTDY	FYPRY	LD CINKYGSPYTKNSGFAT	CVQNLPD

FIGURE 1   Sequence alignment of BF1 (only first 66 residues are shown), bovine protein S, and human Gas6. X refers to γ-carboxyglutamic acid. Numbering is according to Gas6.

was at least 12.5 Å away from the nearest protein atom. All water molecules with oxygen atoms closer than 2.5 Å or with hydrogens closer than 2.0 Å to the nearest protein atom were removed. In the case of protein S, 6067 water molecules were involved in the protein solvation, whereas the Gas6 system had 7063 water molecules. All water molecules were then energy minimized (by 10,000 conjugate gradient steps) at constant volume with the protein held fixed. Belly dynamics was then performed on the water molecules for 20 ps. After reminimizing only the water molecules with 10,000 conjugate gradient steps, the whole system was subjected to minimization at constant volume (another 10,000 conjugate gradient steps). A stepwise heating procedure was implemented over a 5-ps period to bring the system temperature to 300 K, and the trajectory calculations were continued for a period of 25 ps at constant volume and temperature. Each system was then subjected to 50 ps of constant pressure dynamics, which was also disregarded in the trajectory analysis. Subsequently, the integration proceeded for 400 ps. AMBER version 4.1 (Pearlman et al., 1995) was used with the recent AMBER force field (Cornell et al., 1995). The PME method (Essmann et al., 1995) was used to accommodate long-range interactions during dynamics. All covalent bonds involving hydrogens were constrained by a modified form of SHAKE (Hamaguchi et al., 1992). A time step of 1 fs was used in all of the molecular dynamics calculations, and nonbonded interactions were updated at every fifth step throughout the simulation. The final coordinates of both protein S and Gas6 will be deposited in the protein data bank for future use in simulations and experimental data refinements.

RESULTS AND DISCUSSION

Reevaluation of the BF1 system

We present in Fig. 2 the root mean square deviations (RMSDs) of the backbone atoms of BF1 with the defined simulation protocol. A plateau in the RMSD values observed after 120 ps indicates the achievement of stability in the structure near the termination of the trajectory. When considered individually, the Gla and kringle domains displayed similar magnitudes in RMSDs. However, when all of the residues were used in the evaluation of RMSD, a slight increase in the magnitude could be observed. As discussed in earlier simulations (Hamaguchi et al., 1992), such a
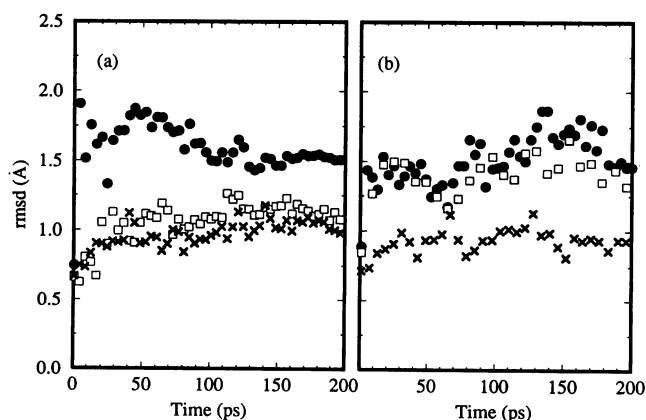
FIGURE 2   Root mean square deviations of the backbone atoms for the BF1 simulation. RMSDs are calculated with respect to the configuration at $t = 0$ ps. ●, All residues; □, residues in the Gla domain; ×, residues in the kringle domain. (a) BF1 calculations with the second generation of AMBER force field (Cornell et al., 1995) and (b) BF1 calculations with the first generation of AMBER force field (Weiner et al., 1984, 1986).

difference in magnitude between the total RMSD and its components from individual domains gives an indication of the interdomain separation. Much larger magnitudes of RMSD reported by Hamaguchi et al. (1992) for residues 1–145 of BF1 may be mainly attributed to the treatments of long-range interactions (a twin-range cutoff in the previous simulation versus the PME method in the present work).

We included in Fig. 2 b the RMSDs of BF1 calculated from the trajectories generated with the first generation of the AMBER force field (Li et al., unpublished results). Because the simulation protocol (including the utilization of the PME method, to account for long-range forces) was identical to the one used in the present simulation, the differences observed in dynamics may be assigned directly to the changes in the force field. Although the total RMSD and the kringle domain component show the same magnitudes as in the previous case, fluctuations around the averages are slightly larger when the first-generation AMBER force field was used. Furthermore, the Gla domain shows higher RMSD values under the first-generation AMBER force field. Similar observations for other proteins were reported in the work of Cornell et al. (1995) due to the change in the force field.

The calcium ion-binding properties of the Gla domain remain largely unchanged. However, there are minor differences in the binding of the N-terminus Ala[1] residue to the protein interior. Hamaguchi et al. (1992) reported that the Gla residues 7, 17, 21, and 27 were hydrogen bonded to Ala[1], whereas Li et al. (1995) found that only the Gla residues 8, 21, and 27 were involved in the bonding. In the present study, the analysis of the structures at the last 20 ps showed that the Gla residues 17, 21, and 27 are found to be hydrogen bonded to Ala[1], as was the case for the x-ray crystal structure of BF1 (Soriano-Garcia et al., 1992). The positions of two calcium ions found near Ala[1] are slightly displaced from the previously reported $N\text{-}Ca^{2+}$ distances of 3.8–3.9 Å (Li et al., 1995) to 4.2 Å. The overall domain structures of BF1 are not affected by the modification of the force field.

Global aspects of the simulations of protein S and Gas6

As was mentioned in the Methodology section, the x-ray crystal structure of BF1 (Soriano-Garcia et al., 1992) was used to model residues 1–47 of protein S and Gas6, and loop searching algorithms were implemented to model the "thumb loops" (the second disulfide loop present after the Gla domain). The major concern here is assurance of the stability of the protein during the dynamical trajectory. The production runs were prepared at constant pressure, which allowed fluctuations in volume, thereby allowing the density to vary naturally until it stabilized. Both the protein S and Gas6 systems reached equilibrium densities around 1.07 and 1.08 g/cc after ~150 ps (data not shown). One measure of the stability of the proteins is obtained from the

RMSDs of backbone atoms as compared to the initial model structure. In Fig. 3, we have depicted the RMSDs of the residues in the Gla domain of protein S and Gas6. Smaller fluctuations in the values of RMSDs of protein S and Gas6 indicate the achievement of stability of the structures upon solvation. The RMSD values are comparable in magnitude with the values of previously studied coagulation proteins for which long-range forces were accommodated (Li et al., 1995, 1996; Wolberg et al., 1996). Although the Gla domains of both protein S and Gas6 were constructed by introducing the appropriate mutations to the corresponding domain of BF1, we find that the RMSDs remain similar for this domain in all three proteins. The additional Ca^{2+} ions do not introduce significant changes to the backbone structure of this region of Gas6.

Comparisons of the average simulation structures for protein S and Gas6 to their $t = 0$ ps models are shown in Figs. 4 and 5, respectively. The final structures from the simulations were also analyzed with the program PROCHECK, a protein analysis program used to test the reasonableness of crystallographic structures (Laskowski et al., 1993). No abnormalities were found in this analysis of the overall structure, bond lengths, bond angles, and dihedral angles for the average simulation structures. The overall averages of the G-factors, which were used in PROCHECK to measure the "normality" of a particular property, are -0.34, -0.41, and -0.72 for protein S, Gas6, and BF1, respectively. Ideally the scores must be above -0.5, and if

FIGURE 4   Ribbon drawing of protein S at $t = 0$ ps, and the structure averaged over the last 20 ps of the 400-ps molecular dynamics (MD) trajectory. The two structures were superimposed, using the best fit of the backbone atoms of the first 32 residues. The last Gla residue (Gla-36) is marked on the structures, along with an asterisk for the N-terminus.

they are below -1.0, PROCHECK suggests further investigation of the structure refinement.

Gla domain structure

Amino acid sequence homology

We first consider the amino acid sequences of the Gla domains of protein S and Gas6 (see Fig. 1) for direct comparisons with the corresponding domain in the solution structure of BF1. In the Gla domain, both protein S and

FIGURE 3   Root mean square deviations of the backbone atoms of the residues in the Gla domain for the Gas6 and protein S simulations. RMSDs are calculated with respect to the configuration at $t = 0$ ps. □, Bovine protein S; ●, human Gas6.
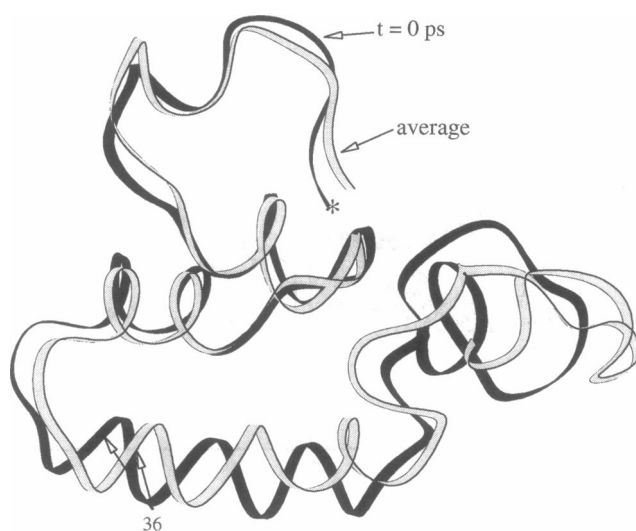
FIGURE 5   Ribbon drawing of Gas6 at $t = 0$ ps, and the structure averaged over the last 20 ps of the 400 ps MD trajectory. The two structures were superimposed using the best fit of the backbone atoms of the first 32 residues. The last Gla residue (Gla-36) is marked on the structures, along with an asterisk for the N-terminus.

Gas6 contain 11 Gla residues, whereas BF1 has 10. In the first 46 residues (up to the "thumb loop") there is 54% sequence identity between protein S and BF1, and 50% between Gas6 and BF1. Protein S and Gas6 have a sequence identity of 67% in the first 46 residues. The positions of the first 10 Gla residues are found to be exactly conserved among the three proteins. The additional Gla residue for protein S and Gas6 is at the same position of the amino acid sequence (Manfioletti et al., 1993). The positions of other basic and acidic groups in this region's sequence are also highly conserved (residues 9, 15, 24, 38, and 43). After placement of the calcium ions, the net charges distributed in region 1–46 were 0, −3, and −2 for BF1, protein S, and Gas6, respectively. (The net charge was zero in all complete simulation systems, even though certain domains may have net charges.) For the three proteins considered in the present study, only BF1 contains an additional basic group (Lys^3) near the N-terminus.

Ala¹ network

The hydrogen bonding interactions of Ala^1 with the interior of the Gla domain are believed to maintain the appropriate shape of the ω-loop (residues 1–11) for prothrombin binding to membrane surfaces. In BF1, Ala^1-N is bound by several hydrogen bonds to Gla^{17}, to the first disulfide loop (Gla^{21} and Pro^{22}), and to the Gla residues immediately following this loop (Gla^{27}). Two calcium ions are also involved in the formation of this network (Table 1). The N-terminus of protein S, in addition to the Gla and calcium contacts, maintains a strong hydrogen bond with Leu^{21} of the first disulfide loop. Although Ala^1-N of Gas6 has only two hydrogen bonds to Gla^{20} and Leu^{21}, it also maintains strong connectivity to the disulfide loop, as has been the

case for the other two proteins. In fact, Ala^1 interacts with Leu^{21} through a bifurcated hydrogen bond in which two hydrogens from the NH_3^+ of Ala^1 participate in the bonding to the oxygen of Leu^{21}. The local calcium ion (4 and ·5) distances to Ala^1-N are similar in BF1 and protein S (Table 1). However, in Gas6, one of the calcium ions (Ca-4) present in the Ala^1 network of BF1 and protein S is somewhat displaced. Furthermore, Ca-5 remains with the N-terminus network but is shifted toward Ala^1-O, whereas Ca-4 is found even closer to this center.

Calcium-Gla network

The arrangement of calcium ions within the Gla domain of BF1 is such that the interionic distances among the neighboring ions are between 4 and 6 Å; this network was found to be stable for the duration of the simulations. The calcium ion network is tightly associated with the Gla residues in this domain. The gross features of this network in protein S and Gas6 are found to be similar to those of BF1 (Table 2). In all cases, the total coordination numbers of the calcium ions (coordination of water molecules, Gla residues, and non-Gla residues) were found to be between 7 and 8. Ions 3, 4, and 5 tend to be the most buried, and ions 1, 2, 6, and 7 are more solvent accessible. More specifically, Ca-4 maintains six ionic bonds with Gla residues in all three proteins. One difference in the calcium network is that Ca-5 makes six ionic contacts in Gas6 as opposed to five in protein S and BF1. Furthermore, Ca-5 forms two non-Gla interactions in Gas6. Those two calcium ions are found to contribute to the previously discussed Ala^1 network. Another dissimilarity is that Ca-3 maintains six Gla coordinations in Gas6 and BF1, as opposed to five for protein S.

We display snapshots of the calcium-Gla network in Fig. 6 (created with the program MOVIEMOL; Hermansson and Ojamae, 1994) for all three systems considered. The snapshots were taken at the termination of each trajectory. Certain ionic bonds found in Table 2 are not seen in the snapshot because the data in this table represent an average over ~30 snapshots. Preservation of the Gla-calcium network among the systems is clearly displayed in the figure, with small differences in the sequence of bonding. Similar minor differences in the Gla-calcium network exist between the current solution structure of BF1 and its crystallographic structure (Soriano-Garcia et al., 1992). The two calcium ions at Gla^{32} and Gla^{36} that were added to neutralize Gas6, do not participate in the existing Ca-Gla network.

We have seen that the Ca-Gla network is largely confined in the solution structures. Furthermore, six calcium ions are confined to a single plane with a RMS deviation of 0.35 Å (see Table 3). To investigate the calcium alignments in the three current simulations, we calculated the displacements (after optimal alignments) of the calcium ions with respect to the x-ray crystal structure of BF1, along with the displacements of calcium ions from the best plane fitted to the first six calcium ions (Table 3). As can be seen from Table 3 A, most of the calcium ions remain relatively close to the

TABLE 1 Comparison of the Ala¹-N network for the predicted solution structures of BF1, bovine protein S, and human Gas6

	Donor	Acceptor	Distance (Å)	Angle (deg)
BF1	Ala^1-N	Gla^{17}-OE3	2.7	111
	Ala^1-N	Gla^{21}-OE4	2.8	168
	Ala^1-N	Pro^{22}-O	2.8	153
	Ala^1-N	Gla^{27}-OE4	2.8	153
	Ala^1-N	Ca-4	4.2	
	Ala^1-N	Ca-5	4.2	
Protein S	Ala^1-N	Gla^6-OE1	2.8	138
	Ala^1-N	Gla^{16}-OE3	2.7	124
	Ala^1-N	Gla^{26}-OE4	2.8	143
	Ala^1-N	Leu^{21}-O	2.9	125
	Ala^1-N	Ca-4	4.1	
	Ala^1-N	Ca-5	4.3	
Gas6	Ala^1-N	Gla^{20}-OE3	2.5	131
	Ala^1-N	Leu^{21}-O	2.9	156
	Ala^1-N	Ca-4	6.3	
	Ala^1-N	Ca-5	4.2	
	Ala^1-O	Ca-4	4.6	
	Ala^1-O	Ca-5	2.5	

The distances and angles were averaged over the last 20 ps of the MD trajectories.

TABLE 2 Ca^{2+}-Gla interactions ($d_{Ca-Gla} \leq 3.0$ Å) for the solution structures of BF1, bovine protein S, and human Gas6

	Gla^6 1234	Gla^7 1234	Gla^{14} 1234	Gla^{16} 1234	Gla^{19} 1234	Gla^{20} 1234	Gla^{25} 1234	Gla^{26} 1234	Gla^{29} 1234	Gla^{32} 1234	Gla^{36} 1234	Water	Other	Total
Ca-1							0110		1010			4		8
							0100		1010			4		7
							0110		1010			3		7
Ca-2		0101					0010	0100	0010			2		7
		0101						0100	0011			3		8
		0100					0011	0100				3		7
Ca-3		0011		1100				1000	0001			2		8
		0011		1100				1000				3		8
		0011		1100				1000	0001			1		7
Ca-4	1000	0010	1010					1001				0	1	7
	1001	0010	1000					1001				1		7
	1000	0010	1010					1001				1		7
Ca-5	0100			0011	0011							3		8
	0100			0011	0011							2		7
	1100			0011	0011							1	2	9
Ca-6					0100	0110						4		7
					1100	0100						5		8
					1100	0100						5		8
Ca-7			0011	0011								3		7
			0011	0011								4		8
			0011	0011								4		8
Ca-8 (Gas6 only)										1100		6		8
Ca-9 (Gas6 only)											0011	4	2	8

Top line, BF1; middle line, bovine protein S; bottom line, human Gas6. The results were averaged over the last 20 ps of the trajectories.

original positions, and those with larger displacements have greater solvent accessibilities. Ca-4 has a slightly modified Gla coordination for Gas6 compared to the other two proteins (see Table 2) and shows a greater displacement. Surprisingly, Ca-7 of BF1 in solution shows larger displacements than for Gas6 and protein S in solution. This large deviation may be due to the electrostatic field exerted by the Arg[55] residue of the thumb loop, which is absent from the latter two systems. It is worth noting that the maximum displacement of a calcium ion in the newly released Factor VIIa x-ray crystal structure (Banner et al., 1996) with respect to the BF1 x-ray crystal configuration is ~0.5 Å.

The first six calcium ions in all three solution systems are confined to a single plane, as was seen for the crystal configuration of BF1. The average displacement (Table 3 B) is slightly smaller for the BF1 solution structure than for its x-ray crystal counterpart. Protein S has the largest average deviation from the plane. The seventh calcium of the protein S solution also lies on the plane, whereas it is somewhat displaced for the other two proteins. The calcium ion (Ca-8) placed near the Gla[32] residue of Gas6 also remains near the plane.

Table 4 contains information on the hydrogen bonds found in the first disulfide loop region. Among the seven H-bonds found in the BF1 loop, three are with Ala[1]-N, and two are with the "thumb loop" (Arg[52] to Gla[20] and Arg[55] to

Gla[20]). Protein S has six H bonds in this region, with Ala[1] connected to the first disulfide loop through one H bond and no direct H-bonds with the "thumb loop." However, Tyr[44] in the connecting region is doubly H-bonded to Cys[22] in protein S. Gas 6 contains seven H bonds in the first disulfide loop region; two have Ala[1]. Cys[17] in the first loop of Gas6 is H-bonded to Tyr[44] as well as to Leu[13]. As in protein S, no H bonds exist between the residues in the first disulfide loop and those in the "thumb loop." Analysis of the H bonds formed among the residues in the Gla domain yielded a total (backbones and side chains) of 27, 30, and 21 interactions for BF1, protein S, and Gas6, respectively. The total number of H bonds involving Gla residues is 20 for both BF1 and protein S and 14 for Gas6 (data not shown). These results imply that for the proteins we have considered in the present study, the Gla residues, a third of the total in the Gla domain, are involved in more than two-thirds of the H bonds found in the domain. Given the differences in the three Gla domain solution structures, it is evident from Fig. 7 that the global secondary structural feature of the Gla domains are preserved.

Phospholipid binding

Because the Gla domains of protein S and Gas6 are similar to BF1 in calcium ion binding and because the secondary
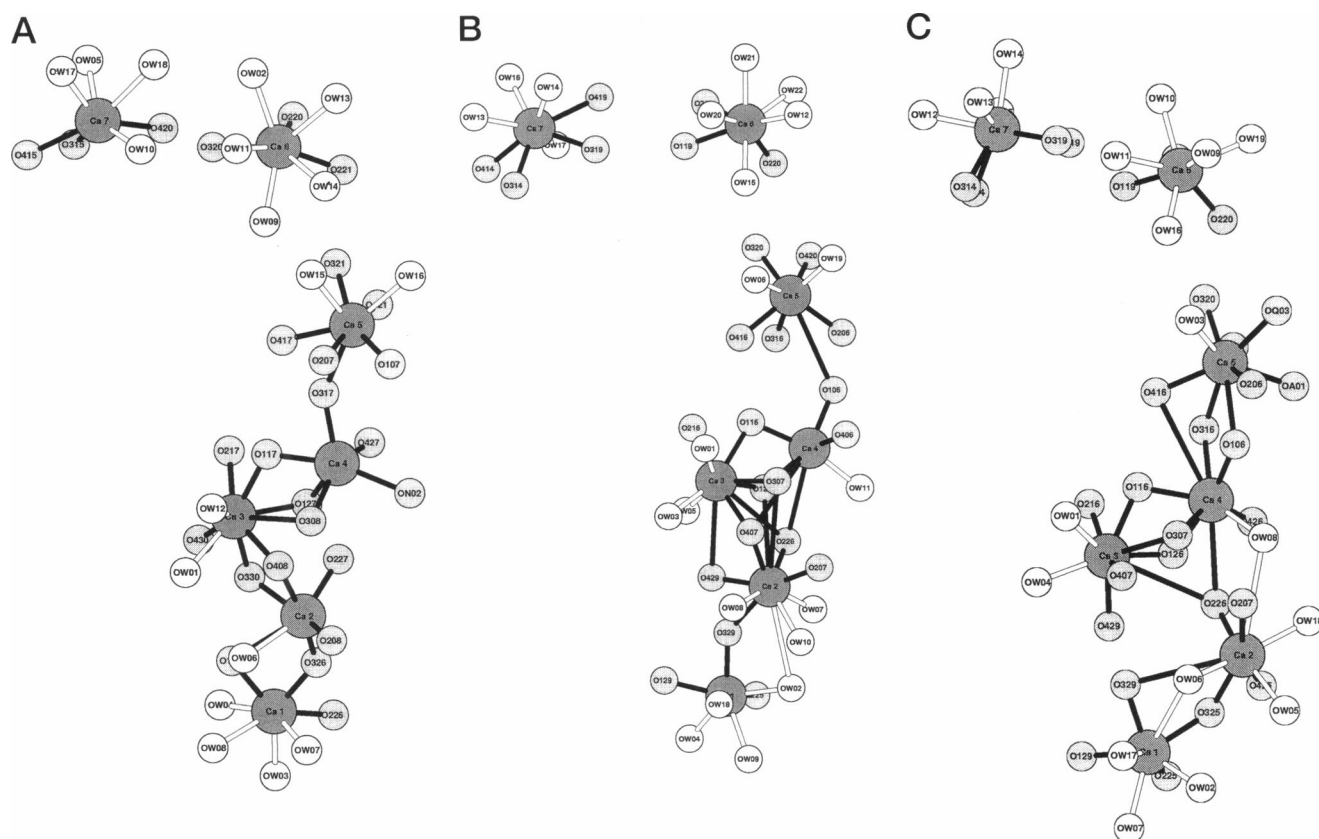
FIGURE 6 Snapshots of the predicted solution structures of the Ca-Gla networks. (a) BF1; (b) bovine protein S; (c) human Gas6. Oxygen atoms from amino acid residues (mainly Gla) are slightly shaded. Unshaded spheres represent oxygens from water molecules. Calcium ions are slightly larger than the oxygens and are shaded. The calcium numbering (1–7) is from Soriano-Garcia et al. (1992). Oxygens from amino acids other than Gla residues carry the single-letter amino acid symbol at the second position from the left. For Gla residues, this position contains carboxylate oxygen labeling (for example, O1, O2, O3, or O4), and W for water. The last two numbers of the oxygen label provide the residue number if the oxygen is from an amino acid.

structures of the Gla domains are largely preserved, we turn to the amino acid sequence details that concern phospholipid binding. Even if the calcium ion-mediated phospholipid binding of the proteins in the coagulation cascade is reported to be associated with the Gla domain, the experimental information regarding the specific binding sites is yet to be discovered. It was proposed (Nelsestuen, 1988) that the phospholipid binding of these proteins is due to the negatively charged Gla region, which can bind to calcium ions coordinated with negatively charged phospholipid molecules (for example, phosphatidylserine). Swairjo et al. (1995) demonstrated that calcium ions coordinated with the phosphatidylserine in a confomationally specific manner provided a bridge for the binding of the protein, anexin V, to the phospholipid surface. For this proposal to be acceptable, calcium ions should have open coordination positions for binding phospholipid while they are bound to the protein (as do calcium ions 1, 6, 7 of the present study; see Table 2). In a later model (Christiansen et al., 1994), the phospholipid binding of the Gla domain is at least partially attributed to the penetration of the hydrophobic residues to the phospholipid upon calcium binding in the Gla domain. For example,

hydrophobic residues of protein C, assumed to be surface exposed, were implicated in the phospholipid binding (Zhang and Castellino, 1994). Li et al. (1995) discussed the homology in the N-terminal ω-loop region of the proteins in the coagulation cascade. The identity of the two residues before the first Gla residue and the two residues after the second Gla residue may be central to the phospholipid binding. Generally, for the vitamin K-dependent coagulation proteins, the first pair (residues 5 and 6 in BF1 numbering; see Fig. 1) consists of two hydrophobic residues except factor IX. The Leu residue at the 5th position is conserved for all vitamin K-dependent coagulation proteins. However, in the case of Gas6, the 5th position is a Phe residue, and this, along with the Val residue at the 4th position, satisfies the proposed hydrophobic condition for phospholipid binding. The second set (residues 8 and 9; Fig. 1) is composed of a hydrophobic residue followed by a hydrophilic one (Arg or Lys), except for factor IX, protein Z, in which both residues are hydrophobic, and protein S, for which both residues are hydrophilic. The hydrophobic residue (or residues) in this set is also believed to be integrated into the lipid surface. Mutation of these residues

TABLE 3 Displacements of calcium ion positions

A. Displacements (after optimal alignment) of calcium ion positions with respect to the corresponding ions in BF1 (crystal) (in Å)

Ca no.	BF1 (solution)	Protein S (solution)	Gas6 (solution)	FVII (crystal)
1	0.82	0.88	0.96	0.40
2	0.79	0.89	0.92	0.16
3	0.43	0.64	0.34	0.22
4	0.51	1.56	0.80	0.42
5	0.97	0.60	0.40	0.43
6	0.25	1.69	0.79	0.54
7	3.01	1.74	1.89	0.21

B. Displacements of calcium ion positions from the best plane fitted to the first six calcium ions.

	BF1 (crystal)	BF1 (solution)	Protein S (solution)	Gas6 (solution)	FVII (crystal)
Avg. deviation*	0.35	0.28	0.66	0.47	0.37
1	0.51	0.12	0.94	0.62	0.55
2	−0.34	0.13	−0.41	0.11	−0.62
3	−0.38	−0.09	−1.11	−0.68	−0.63
4	0.15	−0.09	0.22	−0.19	0.15
5	−0.29	−0.51	−0.12	−0.41	−0.11
6	0.35	0.24	0.48	0.56	0.21
7	3.51	2.31	0.62	3.10	5.16
8				−2.02	
9				5.65	

*Avg. deviation is the average deviation of the first six calcium positions from the best plane.

FIGURE 7 A comparison of the predicted averaged solution structures (over the last 20 ps of the MD trajectories) for residues 1–32 of BF1, protein S, and Gas6. The N-terminus is marked with an asterisk for BF1.

by similar hydrophobic residues led to a small effect on phospholipid binding (for example, mutation of Phe[8] by Leu in human factor IX; Mayhew et al., 1994).

We represent in Fig. 8 ribbon drawings of residues 1–47 of the predicted average solution structures of the three proteins and the x-ray crystal structure of BF1 (Soriano-Garcia et al., 1992). In addition, the planes defined by the best fit to the first six calcium ions in each system, the hydrophobic residues discussed above, and the Gla residues, which do not participate in binding to the first seven calcium ions are included in Fig. 8. In BF1, the previously mentioned three hydrophobic residues (Phe[5], Leu[6], and Val[9]) can be seen to be perpendicular to the plane for both crystal and solution cases and found to be situated at the same distance from the plane, thus facilitating the possible membrane insertion mechanism. Whereas both Leu[4] and Leu[5] for protein S are found to be perpendicular to the plane, only Leu[5] may be more suitable for the insertion because of its extent. Residues Val[4], Phe[5] and Ala[8] for Gas6 are predicted to be aligned approximately for membrane insertion (Fig. 8).

The Gla residues (Gla[33] of BF1; Gla[32] and Gla[36] of protein S and Gas6), which do not participate in the Ca-Gla network, reside near or within a contact distance to the plane. As seen in Fig. 8, Gla[32] of both protein S and Gas6 cuts through the plane, whereas Gla[33] of BF1 and Gla[36] of protein S and Gas6 can directly coordinate with an ion (or atom) that resides on the plane. Thus there is the possibility that these Gla residues participate in membrane binding.

Interestingly, Arg[15], which is conserved in all vitamin K-dependent coagulation proteins (except protein Z, in which it is replaced by another basic residue Lys), has also been shown to participate in phospholipid binding (Zhang et al., 1992). Mutation of Arg[15] to Leu in protein C results in the loss of phospholipid binding. The presence of Arg[15] in Gas6 and the structural similarity in the vicinity of this

TABLE 4 Comparison of intramolecular hydrogen bonds associated with the small disulfide loops of the solution structures of BF1, bovine protein S, and human Gas6

BF1				Bovine protein S				Human Gas6			
Donor	Acceptor	r (Å)	Angle	Donor	Acceptor	r (Å)	Angle	Donor	Acceptor	r (Å)	Angle
Ala[1]-N	Gla[17]-OE4	2.735	111	Ala[1]-N	Leu[21]-O	2.916	125	Ala[1]-N	Gla[20]-OE4	2.458	131
Ala[1]-N	Gla[21]-OE4	2.774	168	Ile[18]-N	Arg[15]-O	2.937	159	Ala[1]-N	Leu[21]-O	2.893	156
Ala[1]-N	Pro[22]-O	2.782	153	Gla[19]-N	Gla[14]-O	3.025	131	Gln[3]-NE	Gla[20]-OE3	2.971	156
Leu[19]-N	Leu[14]-O	2.946	132	Gla[20]-N	Arg[15]-O	3.019	150	Cys[17]-N	Leu[13]-O	2.945	150
Gla[20]-N	Gla[15]-O	2.921	168	Cys[22]-N	Tyr[44]-OH	2.840	167	Gla[19]-N	Gla[14]-O	2.672	162
Arg[52]-N	Cys[18]-O	2.794	148	Tyr[44]-OH	Cys[22]-O	2.717	143	Gla[20]-N	Arg[15]-O	2.956	170
Arg[55]-N	Gla[20]-OE3	2.829	135					Tyr[44]-OH	Cys[17]-O	2.601	170

The results were averaged over the last 20 ps of the MD trajectories. Hydrogen bond criteria used: donor-acceptor distance, <3.10 Å; donor-H $\cdots$ acceptor angle, >110°.
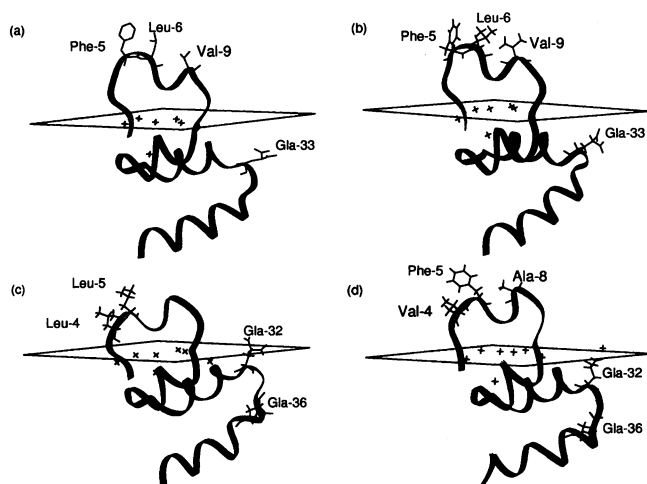
FIGURE 8   Ribbon drawings of the Gla domains of (a) BF1 (in crystal); (b) BF1 (in solution); (c) protein S; and (d) Gas6. The hydrophobic residues believed to be responsible for phospholipid binding are shown. Gla residues that do not participate in Ca-Gla network are also shown, along with the plane determined by the best fit to the first six calcium ions in each system.

residue to BF1 and protein S, which bind to phospholipid surfaces, suggests that Gas6 may likewise bind.

CONCLUSIONS

We have used molecular dynamics simulations to provide estimates for the solution structures of the Gla domain of Gas6 and protein S. Equilibrium structures were obtained and validated with analysis programs.

The secondary structural features of the Gla domains of protein S and Gas6 were found to be conserved when compared with the solution and crystal structures of BF1 in the corresponding region. Furthermore, the network of the N-terminus Ala[1] residue, which is essential for phospholipid binding, was preserved. The Ca^{2+}-Gla network was largely unaltered in the three proteins. The analysis of the Gla domain solution structure and the comparison of the amino acid sequence of Gas6 with the proteins in the coagulation cascade that have high phospholipid binding affinity suggests that the Gla domain of Gas6 fulfills the requirements identified for phospholipid binding.

Note Added in Proof: After our work was completed, we received galley proofs of a related, complementary study of Protein S by Villoutriex et al. to appear in J. Comput. Aided Mol. Des.

REFERENCES

Banner, D. W., A. D'Arcy, C. Chene, F. K. Winkler, A. Guha, W. H. Konigsberg, Y. Nemerson, and D. Kirchhofer. 1996. The crystal structure of the complex of blood coagulation factor VIIa with soluble tissue factor. Nature. 380:41–46.

Christiansen, W. T., A. Tulinsky, and F. J. Castellino. 1994. Functions of individual γ-carboxyglutamic acid (Gla) residues of human protein C. Determination of functionally nonessential Gla residues and correlations with their mode of binding to calcium. Biochemistry. 33:14993–15000.

Cornell, W. D., P. Cieplak, C. I. Bayly, I. R. Gould, K. M. Merz, Jr., D. M. Ferguson, D. C. Spellmeyer, T. Fox, J. W. Caldwell, and P. A. Kollman. 1995. A new force field for molecular mechanical simulation of nucleic acids and proteins. J. Am. Chem. Soc. 117:5179–5197.

Dahlback, B. 1986. Inhibition of protein Ca cofactor function of human and bovine protein S by C4b-binding protein. Biol. Chem. 26:12022–12027.

Dahlback, B., B. Hildebrand, and J. Malm. 1990. Characterization of functionally important domains in human vitamin-K dependent protein S using monoclonal antibodies. J. Biol. Chem. 265:8127–8135.

Dahlback, B., A. Lundwall, and J. Stenflo. 1986. Primary structure of bovine vitamin K-dependent protein S. Proc. Natl. Acad. Sci. USA. 83:4199–4203.

Essmann, U., L. Perera, M. L. Berkowitz, T. Darden, H. Lee, and L. G. Pedersen. 1995. J. Chem. Phys. 103:8577–8593.

Esmon, C. T. 1995. They're not just for clots anymore. Curr. Biol. 5:743–746.

Esmon, C. T., and K. Fukudome. 1995. Cellular regulation of the protein C pathway. Cell Biol. 6:259–268.

Godowsky, P. J., M. R. Mark, J. Chen, M. Sadick, H. Raab, and R. G. Hammonds. 1995. Reevaluation of the roles of protein S and Gas6 as ligands for receptor tyrosine kinase Rse/Tyro 3. Cell. 82:355–358.

Goruppi, S., E. Ruaro, and C. Schneider. 1996. Gas6, the ligand of Axl tyrosine kinase receptor, has mitogenic and survival activities for serum starved NIH3T3 fibroblasts. Oncogene. 12:471–480.

Greengard, J. S., J. A. Fernandez, K-P. Radtke, and J. H. Griffin. 1995. Identification of candidate residues for interaction of protein S with C4b binding protein and activated protein C. Biochem. J. 305:397–403.

Hamaguchi, N., P. Cherifson, T. Darden, L. Xiao, K. Padmanabhan, A. Tulinsky, R. Hiskey, and L. Pedersen. 1992. Molecular dynamics simulations of bovine prothrombin fragment 1 in the presence of calcium ions. Biochemistry. 31:8840–8848.

Hayashi, T., J. Nishioka, and K. Suzuki. 1995. Molecular mechanism of the dysfunction of protein $S_{tokushima}$ ($Lys^{155} \rightarrow Glu$) for the regulation of the blood coagulation system. Biochim. Biophys. Acta. 1272:159–167.

Heeb, M. J., R. M. Masters, J. Rosing, H. M. Bakker, J. A. Fernandes, G. Tans, and J. H. Griffin. 1993. Binding of protein S to factor Va associated with inhibition of prothrombinase that is independent of activated protein C. J. Biol. Chem. 268:2872–2877.

Heeb, M. J., J. Rosing, H. M. Bakker, J. A. Fernandes, G. Tans, and J. H. Griffin. 1994. Protein S binds to and inhibits factor Xa. Proc. Natl. Acad. Sci. USA. 91:2728–2732.

Hermansson, K., and L. Ojamae. 1994. Report UUIC-B19–500. Institute of Chemistry, University of Uppsala, Uppsala, Sweden.

Laskowski, R. A., M. W. MacArthur, D. S. Moss, and J. M. Thornton. 1993. PROCHECK: a program to check the stereochemical quality of protein structures. J. Appl. Crystallogr. 26:283–291.

Li, L., T. Darden, C. Foley, R. Hiskey, and L. Pedersen. 1995. Homology modeling and molecular dynamics simulations of human prothrombin fragment 1. Protein Sci. 4:2341–2348.

Li, L., T. Darden, R. Hiskey, and L. Pedersen. 1996. Homology modeling and molecular dynamics simulations of the Gla domains of human coagulation factor IX and its G[12]A mutant. J. Chem. Phys. 100: 2475–2479.

Lundwall, A., W. Dackowiski, E. Cohen, M. Shaffer, A. Mahr, B. Dahlback, J. Stenflo, and R. Wydro. 1986. Isolation and sequence of the

cDNA for human protein S, a regulator of blood coagulation. *Proc. Natl. Acad. Sci. USA.* 83:6716–6720.

Manfioletti, G., C. Brancolini, G. Avanzi, and C. Schneider. 1993. The protein encoded by a growth arrest specific gene (gas6) is a new member of the vitamin K-dependent proteins related to protein S, a negative coregulator in the blood coagulation cascade. *Mol. Cell Biol.* 13:4976–4985.

Mark, M. R., J. Chen, R. G. Hammonds, M. Sadick, and P. J. Godowsky. 1996. Characterization of Gas6, a member of the superfamily of G domain-containing proteins, as a ligand for Rse and Axl. *J. Biol. Chem.* 271:9785–9789.

Mayhew, M., P. Handford, and G. G. Brownlee. 1994. The binding of natural variants of human factor IX to endothelial cells. *FEBS Lett.* 341:74–78.

Nakano, T., K. Higashino, N. Kikushi, J. Kishino, K. Nomura, H. Fujita, O. Ohara, and H. Arita. 1995. Vascular smooth muscle cell-derived, Gla-containing growth-potentiating factor for Ca^{2+}-mobilizing growth factors. *J. Biol. Chem.* 270:5702–5705.

Nakano, T., K. Kawamoto, J. Kishino, K. Nomura, K. Higashino, and H. Arita. 1997. Requirement of γ-carboxyglutamic acid residues for the biological activity of Gas6: contribution of endogenous Gas6 to the proliferation of vascular smooth muscle cells. *Biochem. J.* 323:387–392.

Nelsestuen, G. L. 1988. Basis for prothrombin-membrane binding. *In* Current Advances in Vitamin K Research. J. W. Suttie, editor. Elsevier Science Publishing, New York.

Ohashi, K., K. Nagata, J. Toshima, T. Nakano, H. Arita, H. Tsuda, K. Suzuki, and K. Mizuno. 1995. Stimulation of Sky receptor tyrosine kinase by the product of growth arrest-specific Gene 6. *J. Biol. Chem.* 270:22681–22684.

Pearlman, D. A., D. A. Case, J. W. Caldwell, W. S. Ross, T. E. Cheatham, III, D. M. Ferguson, L. Seibel, U. C. Singh, P. K. Weiner, and P. A. Kollman. 1995. AMBER 4.1. University of California, San Francisco, CA.

Schwalbe, R. A., B. Dahlback, A. Hillarp, and G. L. Nelsestuen. 1990. Assembly of protein S and C4b-binding protein on membrane. *J. Biol. Chem.* 265:16074–16081.

Schwalbe, R. A., J. Ryan, D. M. Stern, W. Kisie, B. Dahlback, and G. L. Nelsestuen. 1989. Protein structural requirements and properties of membrane binding by γ-carboxyglutamic acid-containing plasma proteins and peptides. *J. Biol. Chem.* 264:20288–20296.

Soriano-Garcia, M., K. Padmanabhan, A. M. de Vos, and A. Tulinsky. 1992. The Ca^{2+} ion and membrane binding structure of the Gla domain of Ca-prothrombin fragment 1. *Biochemistry.* 31:2554–2566.

Stitt, T. N., G. Conn, M. Gore, C. Lai, J. Bruno, C. Radziejewski, K. Mattson, J. Fisher, D. R. Gies, P. F. Jones, P. Masiakowski, T. E. Ryan, N. J. Tobkes, D. H. Chen, P. S. DiStefano, G. L. Long, C. Basillico, M. P. Goldfarb, G. Lemke, D. J. Glass, and G. D. Yancopoulous. 1995. The anticoagulation factor protein S and its relative, Gas6, are ligands for the Tyro 3/Axl family of receptor tyrosine kinases. *Cell.* 80:661–670.

Sugo, T., B. Dahlback, A. Holmgren, and J. Stenflo. 1986. Calcium binding of bovine protein S. *J. Biol. Chem.* 261:5116–5120.

Swairjo, M. A., N. O. Concha, M. A. Kaetzel, J. R. Dedman, and B. A. Seaton. 1995. Ca^{2+}-bridging mechanism and phospholipid head group recognition in the membrane-binding protein annexin V. *Nature Struct. Biol.* 2:968–974.

Varnum, B. C., C. Young, G. Elliott, A. Garcia, T. D. Bartley, Y-W. Fridell, R. W. Hunt, G. Trail, C. Clogston, R. J. Toso, D. Yanagihara, L. Bennett, M. Sylber, L. A. Merewether, A. Tseng, E. Escobar, E. T. Liu, and H. K. Yamane. 1995. Axl receptor tyrosine kinase stimulated by the vitamin K-dependent protein encoded by growth-arrest-specific gene 6. *Nature.* 373:623–626.

Walker, F. J. 1981. Regulation of activated protein C by protein S. *J. Biol. Chem.* 256:11128–11131.

Walker, F. J. 1984. Regulation of vitamin K-dependent protein S, inactivation by thrombin. *J. Biol. Chem.* 259:10335–10339.

Weiner, S. J., P. A. Kollman, D. A. Case, U. C. Sing, C. Ghio, G. Alagona, S. Profeta, Jr., and P. Weiner. 1984. A new force field for molecular mechanical simulation of nucleic acids and proteins. *J. Am. Chem. Soc.* 106:765–784.

Weiner, S. J., P. A. Kollman, D. T. Nguyen, and D. A. Case. 1986. An all atom force field for simulations of proteins and nucleic acids. *J. Comp. Chem.* 7:230–252.

Wolberg, A. S., L. Li, W-F. Cheng, N. Hamaguchi, L. G. Pedersen, and D. W. Stafford. 1996. Characterization of γ-carboxyglutamic acid residue 21 of human factor IX. *Biochemistry.* 35:10321–10327.

Zhang, L., and F. J. Castellino. 1994. The binding energy of human coagulation protein C to acidic phospholipid vesicles contains a major contribution from leucine 5 in the γ-carboxy glutamic acid domain. *J. Biol. Chem.* 269:3590–3595.

Zhang, L., A. Jhingan, and F. J. Castellino. 1992. Role in individual γ-carboxyglutamic acid residues of activated human protein C in defining its in vitro anticoagulant activity. *Blood.* 80:942–952.